

1 **Increase of dissolved inorganic carbon and decrease of pH in near surface**
2 **waters of the Mediterranean Sea during the past two decades**

3

4

5 Liliane. Merlivat ^a, Jacqueline. Boutin ^a, David. Antoine ^{b,c}, Laurence. Beaumont ^d, Melek.
6 Golbol ^b, Vincenzo. Vellucci. ^b

7

8 ^a Sorbonne Universités (UPMC, Univ Paris 06)-CNRS-IRD-MNHN, LOCEAN Laboratory,
9 F-75005 Paris, France

10 ^b Sorbonne Universités (UPMC, Univ Paris 06)-CNRS, LOV, Observatoire Océanologique,
11 Villefranche-sur-Mer 06230, France

12 ^c Remote Sensing and Satellite Research Group, Department of Physics and Astronomy,
13 Curtin University, Perth, WA 6845, Australia

14 ^d Division Technique INSU-CNRS, 92195 Meudon Cedex, France

15

16 Corresponding author: L. Merlivat (merlivat@locean.upmc.fr)

17

18

19 **Abstract**

20 Two three-year-long time series of hourly measurements of the fugacity of CO₂ (fCO₂) in the
21 upper 10m of the surface layer of the northwestern Mediterranean Sea have been recorded by
22 CARIOCA sensors almost two decades apart, in 1995-1997 and 2013-2015. By combining
23 them with alkalinity derived from measured temperature and salinity, we calculate changes of
24 pH and dissolved inorganic carbon (DIC). DIC increased in surface seawater by ~ 25 μmol
25 kg⁻¹ and fCO₂ by 40 μatm, whereas seawater pH decreased by ~ 0.04 (0.0022 yr⁻¹). The DIC
26 increase is about 15% larger than expected from equilibrium with atmospheric CO₂. This
27 could result from natural variability, e.g. the increase between the two periods in the
28 frequency and intensity of winter convection events. Likewise, it could be the signature of the
29 contribution of the Atlantic Ocean as a source of anthropogenic carbon to the Mediterranean
30 Sea through the strait of Gibraltar. Under this assumption, we estimate that the part of DIC
31 accumulated over the last 18 years represents ~30% of the total change of anthropogenic

32 carbon since the beginning of the industrial period.

33

34 **1 Introduction**

35 The concentration of atmospheric carbon dioxide (CO₂) has been increasing rapidly over
36 the 20th century and, as a result, the concentration of dissolved inorganic carbon (DIC) in
37 the near surface ocean increases, which drives a decrease in pH in order to maintain a
38 chemical equilibrium. These changes have complex direct and indirect impacts on
39 marine organisms and ecosystems [Gattuso and Hansson, 2011]. Empirical methods to
40 estimate the anthropogenic CO₂ penetration in the ocean since the industrial revolution
41 have improved over the past few decades [Chen and Millero, 1979; Gruber et al., 1996];
42 [Sabine et al., 2008]; [F Touratier and Goyet, 2004; 2009; Woosley et al., 2016]. As the
43 concentration of anthropogenic carbon, C_{ant}, cannot be distinguished from the natural
44 background of DIC through total DIC measurements, these methods are based on the
45 analysis of different chemical properties of the water column. Direct estimates of the
46 anthropogenic CO₂ absorption in the sea surface layers are difficult owing to the large
47 natural variability driven by physical and biological phenomena. [Bates et al., 2014] have
48 extracted the trend from the large variability, based on analysis of a long time series
49 (monthly or seasonal sampling). For the global surface ocean, [Lauvset et al., 2015] have
50 used the Surface Ocean CO₂ Atlas (SOCAT) database [Bakker et al., 2014] combined with
51 an interpolation method. Estimates of anthropogenic storage in the Mediterranean Sea
52 differ by about a factor of two [Huertas et al., 2009; F Touratier and Goyet, 2009]. In
53 addition to the anthropogenic signal, oceanic DIC can also be the signature of a strong
54 interannual variability. In the North Atlantic, for instance, McKinley et al. [2011] has
55 shown that the long term trend emerges after more than 25 years because of natural
56 variability.

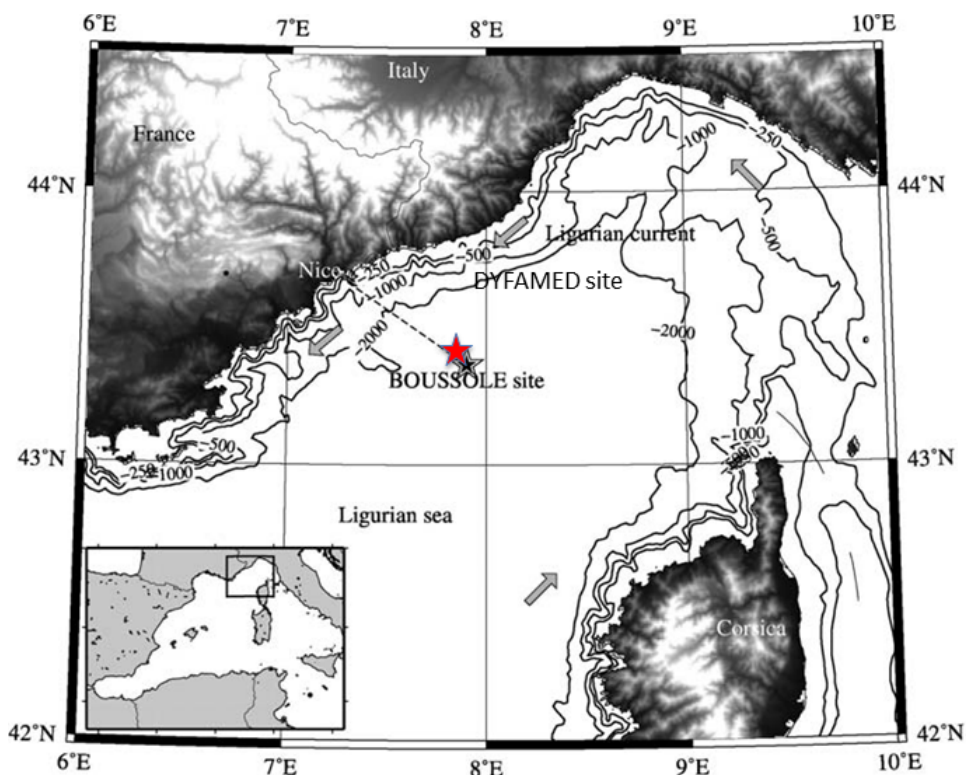
57 A high frequency sampling of the seawater carbon chemistry at the air-water interface over
58 extended periods of time is useful to assess trends and variability of DIC. In this paper we
59 analyze two three-year time series of hourly fugacity of CO₂, fCO₂, measured with
60 autonomous CARIOCA sensors [Copin-Montégut et al., 2004; Merlivat and Brault, 1995] in
61 1995-1997 and 2013-2015, at two nearby locations in the northwestern Mediterranean Sea
62 (Fig. 1). Using measured fCO₂, temperature (T) and salinity (S), we derive the other variables
63 of the carbonate system (pH and DIC). The experimental setting is first described, and the

64 recent data obtained over the 2013-2015 period are presented. Combined with the 1995-1997
65 measurements previously published [Hood and Merlivat, 2001], we estimate the decrease of
66 pH and the increase of DIC. The results are discussed with respect to the contributions of the
67 exchange with atmospheric CO₂, to the possible impact of vertical mixing and to recent
68 estimates of the transport of anthropogenic carbon from the Atlantic Ocean over a 18 years
69 period.

70

71 2 Material and methods

72 2.1-The BOUSSOLE and DYFAMED sites



73

74 Fig.1. The area of the northwestern Mediterranean Sea showing the southern coast of France,
75 the Island of Corsica, the main current branches (gray arrows), and the location of the
76 DYFAMED site (43°25'N, 7°52'E, red star) and the BOUSSOLE buoy (43°22'N, 7°54'E,
77 black star) in the Ligurian Sea.

78

79 Data collection was carried out at the BOUSSOLE site (43°22'N, 7°54'E) in 2013-2015
80 [Antoine et al., 2008; Antoine. and others, 2006] and at the DYFAMED site (43°25'N,
81 7°52'E) in 1995-1997 [J.C. Marty et al., 2002]. These sites are 3 nautical miles apart, both
82 located in the Ligurian Sea, one of the basins of the northwestern Mediterranean Sea (Fig.1).
83 The water depth is of ~2400 m. The prevailing ocean currents are usually weak ($<20 \text{ cm s}^{-1}$),

84 because these sites are in the central area of the cyclonic circulation that characterizes the
85 Ligurian Sea. The two sites surrounded by the permanent geostrophic Ligurian frontal jet
86 flow are protected from coastal inputs [Antoine et al., 2008; Heimbürger et al., 2013; Millot,
87 1999]. Monthly cruises are carried out at the same location .

88

89 2.2- Analytical methods

90 At DYFAMED, $f\text{CO}_2$ measurements at 2 m were provided by an anchored floating buoy
91 fitted with a CARIOCA sensor. At BOUSSOLE, measurements were carried out from a
92 mooring normally dedicated to radiometry and optical measurements, and onto which two
93 CARIOCA sensors were installed. Both monitored $f\text{CO}_2$ hourly at 3 and 10 m depth (although
94 only one of the two depths was equipped with a functional sensor at some periods); S and T
95 were monitored at the same two depths using a Seabird SBE 37-SM MicroCat instrument.
96 The CARIOCA sensors were adapted to work under pressure in the water column. They were
97 swapped about every 6 months, with serviced and calibrated instruments replacing those
98 having been previously deployed. The accuracy of CARIOCA $f\text{CO}_2$ measurements by the
99 spectrophotometric method based on the optical absorbance of a solution thymol blue diluted
100 in seawater is estimated at $2 \mu\text{atm}$ during both periods. Hood and Merlivat [2001] have
101 reported agreement between $f\text{CO}_2$ measured by CARIOCA buoys, similar to the one deployed
102 at DYFAMED, with ship based measurements, during a number of field programs, with an
103 accuracy of $2 \mu\text{atm}$ and a precision of $5 \mu\text{atm}$.

104 At Boussole, newly designed $f\text{CO}_2$ sensors have been calibrated using in situ seawater
105 samples taken at 5 and 10 m depth during the monthly servicing cruises to the mooring. The
106 total alkalinity, Alk, and DIC of the samples were determined by potentiometric titration
107 using a closed cell according to the method developed by [Edmond, 1970]. Certified
108 Reference Materials (CRMs) supplied by Dr. A.G. Dickson (Scripps Institution of
109 Oceanography, San Diego, USA) were used for calibration [Dickson et al., 2007]. The
110 accuracy is estimated at $3 \mu\text{mol kg}^{-1}$ for both DIC and Alk. $f\text{CO}_2$ is calculated using the
111 dissociation constants of Mehrbach refitted by Dickson and Millero [Dickson and Millero,
112 1987; Mehrbach et al., 1973] as recommended by Alvarez et al.[2014] for the Mediterranean
113 Sea. Error on $f\text{CO}_2$ derived from an individual sample is expected to be on the order of 5
114 μatm [Millero, 2007]. About 8 samples have been used to calibrate each CARIOCA sensor so
115 that the error on the absolute calibration of each $f\text{CO}_2$ CARIOCA sensor, is estimated at 1.8
116 μatm . In addition, we observe that the standard deviation of the difference between the
117 CARIOCA $f\text{CO}_2$ and $f\text{CO}_2$ computed with the monthly discrete samples (Fig. 2b) is equal to

118 4.4 μatm , consistent with the expected precision on CARIOCA $f\text{CO}_2$ of 5 μatm . Alk and S of
 119 the 56 samples taken at BOUSSOLE are linearly correlated according the following
 120 relationship :

$$121 \quad \text{Alk} (\mu\text{mol kg}^{-1}) = 87.647 S - 785.5 \quad (1)$$

122 The standard deviation of the Alk data around the regression line is equal to 4.4 $\mu\text{mol kg}^{-1}$
 123 ($r^2=0.89$).

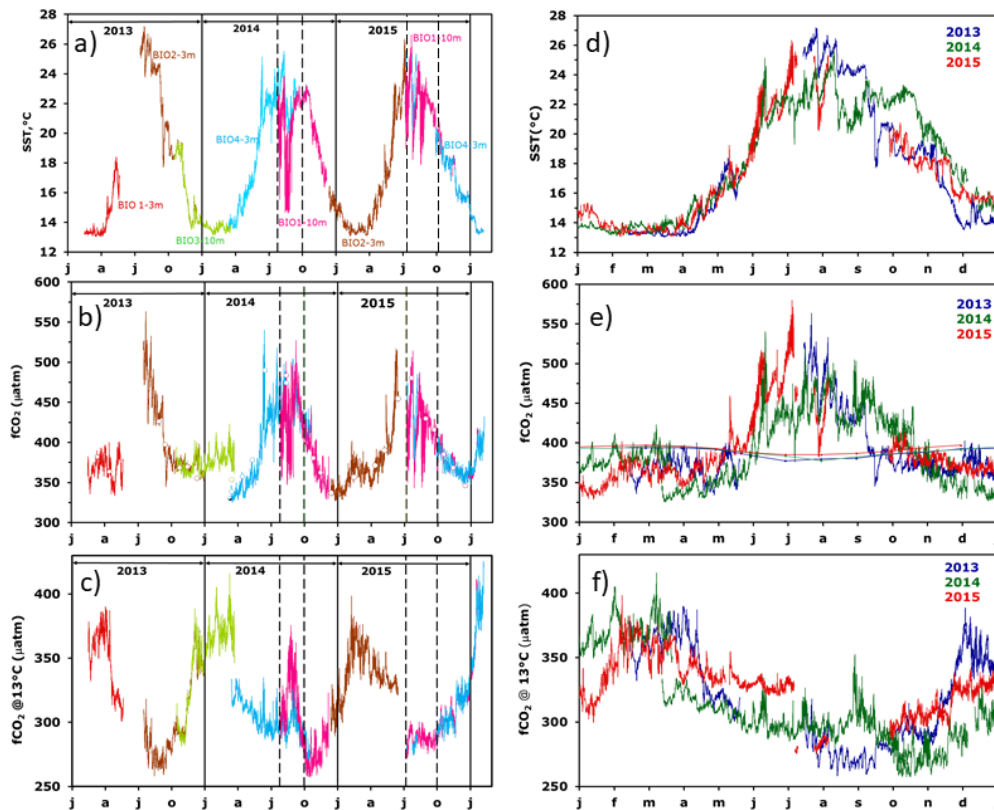
124

125 3 Results

126 3.1 The BOUSSOLE mooring (2013-2015) time series

127 Temperature and $f\text{CO}_2$ were measured from February 2013 to February 2016. All seasons
 128 were well represented, with missing data only in May-July 2013. For some periods,
 129 simultaneous measurements were made at 3 and 10 m depth (Fig. 2, a, b, c).

130



131

132 Fig.2. Interannual variability of CARIOCA data: a) T, b) $f\text{CO}_2$, c) $f\text{CO}_2@13$. The dotted lines
 133 indicate the period affected by stratification and internal waves (July, 26th to October 1st,
 134 2014 and July, 8th to October 1st, 2015). On 2(b), the open circles correspond to $f\text{CO}_2$ data
 135 derived from DIC and alkalinity measurements of samples taken at 5 and 10 m. (d), (e), (f),

136 seasonal variability. On 2(e), the thin lines indicate $f\text{CO}_{2\text{atm}}$. Note that the color code on (d),
137 (e), (f) is different from (a), (b), (c).

138

139 The range of temperature (Fig. 2a) extends from 13°C in winter up to 27°C in summer,
140 followed by progressive cooling in fall. The coldest temperature, 13°C, results from the
141 winter vertical mixing with the deeper Levantine Intermediate Water, LIW, marked by
142 extrema in temperature and salinity [Copin-Montegut and Begovic, 2002]. Temperature
143 provides the main control of the seasonality of $f\text{CO}_2$, from 350 μatm to more than 550 μatm in
144 summer 2013 (Fig. 2b). The fugacity of CO_2 in seawater is a function of temperature, DIC,
145 alkalinity, salinity and dissolved nutrients. In the oligotrophic surface waters of the
146 Mediterranean Sea, the effect of nutrients may be neglected. Temperature and DIC have the
147 strongest influences. By normalizing $f\text{CO}_2$ to a constant temperature, the thermodynamic
148 effect can be removed and changes in $f\text{CO}_2$ resulting from changes in DIC can be more easily
149 identified. Figure 2c shows the variability of $f\text{CO}_2$ normalized to the constant temperature of
150 13°C, ($f\text{CO}_2@13$), using the equation of [Takahashi *et al.*, 1993]. The underlying processes
151 that govern the seasonal variability of $f\text{CO}_2@13$ are successively winter mixing, biological
152 activity (organic matter formation and remineralization) and deepening of mixed layer in fall
153 [Begovic and Copin-Montegut, 2002; Hood and Merlivat, 2001]. Biology accounts for the
154 decline in $f\text{CO}_2@13$ observed from March-April to late summer; the ensuing increase of
155 surface $f\text{CO}_2@13$ is associated with the deepening of the mixed layer in the fall or convection
156 in winter as the vertical distribution of $f\text{CO}_2@13$ at DYFAMED shows a maximum in the 50-
157 150 m layer where a large remineralization of organic matter occurs, the productive layer
158 being mostly between 0 and 40 m [Copin-Montegut and Begovic, 2002]. The contribution of
159 air-sea exchange is not significant [Begovic and Copin-Montegut, 2002]. Over the period
160 2013-2015, the CO_2 air-sea flux from the atmosphere to the ocean surface is equal to -0.45
161 $\text{mol m}^{-2} \text{yr}^{-1}$.

162 During summer 2014, large differences between measurements at 3 and 10 m were
163 observed (Fig. 2, a, b, c between dashed lines). A detailed analysis of the temporal
164 variability during that period underscores the role of inertial waves at the frequency of
165 17.4 hours that create the observed differences between the 2 depths of observations,
166 the deeper waters being colder and enriched in $f\text{CO}_2@13$. T and $f\text{CO}_2@13$ variability is
167 dominated by inertial waves. In particular, from 15 to 26 of August 2014, the difference

168 in T between the two depths is as large as 7.6°C, and 5.1°C on average. fCO₂ decreases on
169 average by 32.7 μatm leading to an increase of fCO₂@13 equal to 42.8 μatm.
170 The 2013-2015 seasonal and inter-annual variability of T, fCO₂ and fCO₂@13 is
171 illustrated on Fig. 2, d, e, f. The larger interannual changes in temperature (Fig.2, d) are
172 observed during summer, both at 3 m and 10 m depth, while over February and March, a
173 constant value of 13°C is observed as the result of vertical mixing with the LIW. A very
174 large inter-annual variability of fCO₂@13 is observed for T<14°C (Fig. 2,f). This is
175 associated with the winter mixing at the mooring site, which is highly variable from year
176 to year. Winter mixed-layer depth, MLD, varies between 50 and 160 m, at the top of the
177 LIW over the 2013-2015 period [Coppola *et al.*, 2016]. The variable depth of the winter
178 vertical mixing causes the difference in fCO₂@13 as fCO₂ increases with depth [Copin-
179 Montegut and Begovic, 2002]. The deepening of MLD is driven by episodic and intense
180 mixing processes characterized by a succession of events lasting several days, related to
181 atmospheric forcing [Antoine *et al.*, 2008] which lead to increase in fCO₂@13. Figure 2,e
182 illustrates the solubility control of the variability of fCO₂, as fCO₂ increases when T
183 increases. Another cause of inter-annual variability of fCO₂ for T~14°C is the timing of
184 the spring increase of biological activity which differs by a month between years; for
185 instance, it happened at the beginning of April in 2013, T~15-16°C and by mid March in
186 2014, T~14°C. Another cause is the deepening of the mixed layer due to the fall cooling
187 which varies by a month between years.

188

189 **3.2 Decadal changes of hydrography**

190 **3.2.1 Sea surface temperature changes**

191 Monthly mean values of temperature have been computed for the two three-year periods,
192 1995-1997 and 2013-2015. In 1995-1997, fCO₂ and T at 2 m were measured with CARIOCA
193 sensors installed on a buoy at DYFAMED [Hood and Merlivat, 2001]. The mean annual
194 temperature of hourly CARIOCA data is equal to 18.21°C. For 2013-2015, temperature
195 measurements made on the BOUSSOLE mooring at 3 and 10 meters have been used. For the
196 April to September time interval, there are only data at 3m depth. In addition, temperature
197 data measured half hourly at 0.7 m at a nearby meteorological buoy (43°23'N, 7°50'E)
198 (<http://www.meteo.shom.fr/real-time/html/DYFAMED.html>) have been used (Fig.3d). Mean
199 annual temperature are equal to 18.29°C and 17.97°C respectively, based on the
200 meteorological buoy and the BOUSSOLE mooring data. The two sets of data differ

201 essentially during July and August, with the temperatures at 3 m being colder than at 0.7 m,
202 indicating a thermal gradient between the two depths during summer. Therefore, for 2013-
203 2015, we select the mean annual value computed with the meteorological buoy, 18.29°C, as
204 better representing the sea surface. This value is very close to 18.21°C computed for 1995-
205 1997. Then, no significant change of SST is found between the 2 decades, with a mean value
206 equal to 18.25°C.

207 **3.2.2** Sea surface salinity changes

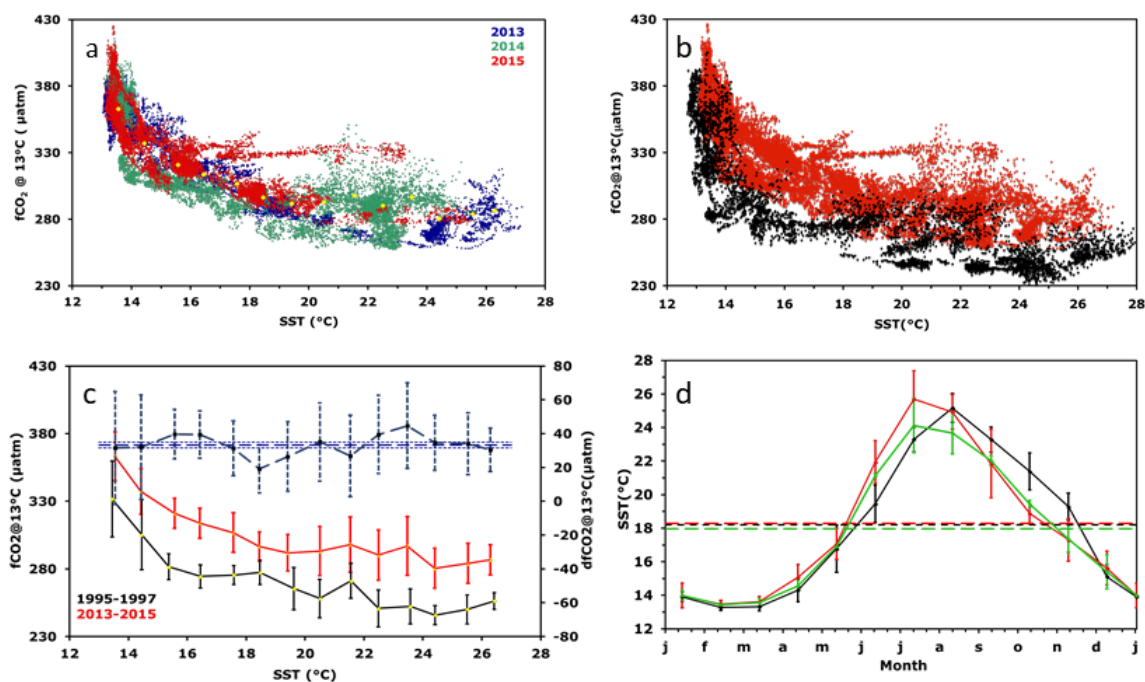
208 The mean value of salinity computed from 56 samples taken at BOUSSOLE in 2013-2015 is
209 equal to 38.19+/-0.14. In 1998-1999, ship measurements of surface salinity were made during
210 monthly cruises at the DYFAMED site [*Copin-Montégut et al.*, 2004]. The mean salinity of
211 this set of 19 data is equal to 38.21+/-0.12. Thus, there is no significant salinity change
212 between the two decades.

213

214 **3.3** Decadal changes of fCO₂@13

215 **3.3.1** Time series of fCO₂@13 in 1995-1997 and 2013-2015

216 The two time series of high frequency data were analyzed in order to quantify the change of
217 fCO₂@13 at the sea surface two decades apart. To account for the interannual seasonal
218 variability as well as irregular sampling, we performed an analysis of the change of fCO₂@13
219 as a function of SST (Fig. 3, a and b). For the 2013-2015 data set, we excluded summer data
220 measured at 10 m depth as they were not representative of the surface mixed layer due to a
221 strong stratification. Much larger fCO₂@13 values are observed at low temperature than at
222 high temperature, the decrease being similar for the two studied periods and strongly non
223 linear. As described in section 3.1, large values at low temperature result from mixing with
224 enriched deep waters during winter and low values for 26°C-28°C temperatures occur at the
225 end of summer after biological drawdown of carbon. An increase of fCO₂@13 between the 2
226 periods is clearly highlighted for the whole range of temperature.



227
 228 Fig.3. (a) $fCO_2@13$ as a function of temperature for hourly data in 2013, 2014 and 2015. The
 229 yellow dots indicate mean $fCO_2@13$ (b) as in (a) but for all hourly data in 1995-1997 (black)
 230 and in 2013-2015 (red) (c) As in (b), but for average values per $1^\circ C$ interval (standard
 231 deviation as dotted line). The difference between the two periods is also displayed (dashed
 232 black curve; scale on the right axis). (d) Mean monthly sea surface temperature for 1993-1995
 233 (black curve; CARIOCA sensors), 2013-2015 (green; CARIOCA sensors), 2013-2015 (red,
 234 meteorological buoy). Corresponding mean annual values are indicated by dotted lines.

235
 236 **3.3.2 Trend analysis and statistics**

237 To quantify the change of $fCO_2@13$ between the two data sets, we proceed as follows: data
 238 are binned by $1^\circ C$ temperature intervals, thereby removing any potential seasonal weighting,
 239 especially towards the $13-14^\circ C$ winter months temperature. The measurements made in this
 240 temperature interval represent about 25% of the total number of data for both periods. For
 241 each of the fourteen $1^\circ C$ step, the mean and standard deviation of hourly $fCO_2@13$
 242 measurements are reported in Table 1 and on Fig. 3c.

243
 244
 245
 246

Time interval 1995-1997				Time interval 2013-2015				Temporal change	
T ¹ °C	fCO ₂ @13 μatm	N	standard deviation μatm	T ¹ °C	fCO ₂ @13 μatm	N	standard deviation μatm	dfCO ₂ @13 μatm	standard deviation μatm
13.45	331.58	1212	28.09	13.55	363.14	6869	18.07	31.56	33.40
14.45	305.28	495	26.02	14.43	337.16	3270	16.65	31.87	30.89
15.37	281.54	447	9.62	15.57	321.10	3112	11.09	39.56	14.68
16.44	274.43	182	8.53	16.42	313.79	1818	11.09	39.36	13.99
17.58	275.54	190	7.04	17.56	306.83	1528	14.65	31.29	16.25
18.47	277.34	300	9.04	18.45	296.57	2621	10.95	19.23	14.20
19.62	265.43	342	15.58	19.41	291.84	1406	13.45	26.40	20.59
20.50	258.08	529	14.15	20.50	293.16	1135	18.21	35.08	23.06
21.56	271.15	239	12.98	21.54	297.96	1200	20.41	26.82	24.19
22.49	250.75	742	13.66	22.49	290.27	2385	18.57	39.52	23.05
23.57	252.22	320	13.00	23.47	296.92	747	21.77	44.70	25.36
24.41	245.85	506	7.08	24.40	280.44	959	14.82	34.59	16.43
25.50	250.06	215	10.77	25.53	284.05	456	14.81	33.99	18.31
26.42	256.29	279	6.24	26.29	286.71	249	11.23	30.42	12.85

247

248

Table 1:

249 Distribution of temperature, fCO₂@13, and increase dfCO₂@13 data binned by 1°C
250 temperature interval for the 2 periods 1995-1997 and 2013-2015.

251 The mean temperature within each 1° step differ for the two periods as the distribution of
252 individual measurements are not identical.

253 For both data sets, a monotonic relationship between fCO₂@13 and T is observed with
254 correlation coefficients respectively equal to -0.861 and -0.857. The difference in fCO₂@13
255 between the two periods, dfCO₂@13, is derived in each temperature step, as the difference
256 between column 2 and 6 of Table 1. The variability of this difference is estimated as the
257 quadratic mean of the standard deviation in each time series. Both values are reported in
258 Table 1, column 9 and 10, and on Fig. 3c.

259 The distribution of dfCO₂@13 values around the mean seems random and indicates no

260 trend dependency with SST (Fig. 3c). This suggests that the processes which control the
261 seasonal variation of $f\text{CO}_2@13$ at the sea surface have not changed over the last two
262 decades.

263 We have estimated the uncertainties in the estimates of the difference $df\text{CO}_2@13$ with 2
264 methods. Firstly, the arithmetic mean of $df\text{CO}_2@13$ is equal to $33.17\mu\text{atm}$, with a standard
265 deviation, SD, and standard error, SE, respectively equal to $6.29\mu\text{atm}$ and $1.68\mu\text{atm}$. A 95%
266 confidence interval is thereby achieved within 1.96 SE, i.e. $3.29\mu\text{atm}$. A second approach
267 consists of computing a weighted average of the mean of $df\text{CO}_2@13$. In this case, mean
268 weighted value of $df\text{CO}_2@13$ over the whole range of temperature is estimated, the weights
269 being equal to the variance of $df\text{CO}_2@13$ in each temperature step. It is equal to $32.70\mu\text{atm}$.
270 The weighted SD, and the associated SE, of the 14 data points are respectively equal to 4.85
271 μatm and $1.30\mu\text{atm}$. A 95% confidence interval is achieved within $2.54\mu\text{atm}$. The difference
272 between the two mean $df\text{CO}_2@13$ estimates is $0.47\mu\text{atm}$, well below SE. In the following,
273 we have chosen the former method which produces a more conservative estimate.

274

275 3.4 Changes of seawater carbonate chemistry in surface waters

276 We estimated the DIC and pH changes related to the increase of $f\text{CO}_2@13$ measured at the
277 sea surface 18 years apart, assuming a mean salinity equal to 38.2, a mean alkalinity equal to
278 $2562.3\mu\text{mol kg}^{-1}$ following equation (1), and a mean in situ temperature, T, equal to
279 18.25°C . The dissociation constants of Mehrbach refitted by Dickson and Millero [*Dickson*
280 *and Millero*, 1987; *Mehrbach et al.*, 1973] were used. pH is calculated on the seawater scale.
281 The error on $df\text{CO}_2@13$, $\pm 3.3\mu\text{atm}$, has been propagated to compute the uncertainty on
282 $d\text{DIC}$ and $dp\text{H}_{\text{SWS}}$. This makes the implicit assumption that there is no systematic error on
283 DIC and $p\text{H}_{\text{SWS}}$ derived from $f\text{CO}_2@13$ between the two time periods; in particular, mean
284 temperature and salinity remain the same (section 3.2). This is further discussed in section
285 4.1. We compute an increase of DIC, $d\text{DIC}$, equal to $25.2\pm 2.7\mu\text{mol kg}^{-1}$ (1.40 ± 0.15
286 $\mu\text{mol kg}^{-1}\text{yr}^{-1}$) and the decrease of $p\text{H}_{\text{SWS}}$, $dp\text{H}_{\text{SWS}}$ equal to $-0.0397\pm 0.0042 p\text{H}_{\text{SWS}}$ unit ($-$
287 $0.0022\pm 0.0002 p\text{H}_{\text{SWS}}$ unit yr^{-1}) (Table 2).

288
289
290
291
292
293
294
295

	d fCO ₂ [*] @ 13 µatm	d fCO ₂ [*] @ T µatm	d DIC [*] µmolkg ⁻¹	d pH _{SWS} ^{***} pH unit	dfCO ₂ @T annual µatm yr ⁻¹	d DIC annual µmolkg ⁻¹ yr ⁻¹	d pH _{SWS} ^{***} annual pH unit yr ⁻¹
sea surface	33.2 +/-3.3	41.4 +/-4.1	25.2 +/-2.7	-0.0397 +/-0.0042	2.30 +/-0.23	1.40 +/-0.15	-0.0022 +/-0.0002
atmosphere Lampedusa data		34.3 +/-2.3	**20.8 +/-1.3		1.91 +/-0.13	1.15 +/-0.07	
dfCO ₂ @T _{air} /dfCO ₂ @T _{sea}		0.83 +/-0.10	0.83 +/-0.09				

296

297

Table 2

298 Seasonally detrended long term and annual trends of seawater carbonate chemistry and
299 atmosphere composition.

300 T, mean annual temperature equal to 18.25°C

301 *, change from 1995-1997 to 2013-2015.

302 **, dDIC_{ant}

303 *** dpH_{SWS} computed at T

304

305 3.5 Changes in atmospheric and seawater fCO₂

306 The increase of atmospheric fCO₂ from 1995-1997 to 2013-2015 was computed from
307 monthly atmospheric xCO₂ concentrations measured at the Lampedusa Island station (Italy)
308 (35°31'N, 12°37'E) (<http://ds.data.jma.go.jp/gmd/wdcgg/>) (see equation 3 in [*Hood and*
309 *Merlivat*, 2001]). Considering a mean annual in situ temperature equal to 18.25°C and an
310 atmospheric pressure of 1 atm, we derived a mean atmospheric fCO₂ equal to 355.3+/-0.8
311 µatm for 1995-1997 and 389.6+/-0.9 µatm for 2013-2015, that is an increase of 34.3+/-2.3
312 µatm (95% confidence interval) (Table 2). At this temperature, the change of fCO₂ at the sea
313 surface is 41.4+/-4.1 µatm. Thus the contribution of the increase in atmospheric CO₂ is
314 responsible for 84+/-5 % of the increase of fCO₂ measured in the surface waters. With the
315 same salinity and alkalinity as previously, the corresponding change in surface DIC, assuming
316 air-sea equilibrium, would be 20.8+/- 1.3 µmol kg⁻¹ (Table 2).

317

318 4 Discussion

319 4.1 Time change of surface alkalinity

320 High frequency measurements of $f\text{CO}_2$ and temperature over 2 periods of 3 years, 2 decades
321 apart, have allowed the computation of an increase of DIC equal to $25.1\pm 2.3 \mu\text{mol kg}^{-1}$
322 assuming no change of alkalinity. In the range of salinity of the BOUSSOLE samples, 37.9 to
323 38.5, the alkalinity values computed with Eq (1) are larger than those predicted by the
324 relationship established for the DYFAMED site, with a mean difference equal to $10\pm 2 \mu\text{mol}$
325 kg^{-1} [Copin-Montegut and Begovic, 2002]. In both cases alkalinity measurements were made
326 with a potentiometric method using certified reference material supplied by A.G. Dickson for
327 calibration. It is difficult to identify the cause for a possible change of alkalinity between the 2
328 periods, 18 years apart, while no salinity change has been observed. At a coastal site 50 km
329 away from DYFAMED, Kapsenberg et al. [2017] have measured an increase of alkalinity
330 unrelated to salinity over the period from 2007 to 2015. They attribute it to changes in
331 freshwater inputs from land. However, based on data from Coppola et al. [2016], alkalinity in
332 the upper 50m at DYFAMED did not change significantly from 2007 through 2014 (3.204
333 $\mu\text{mol kg}^{-1}$, $P=0.0794$, $r^2=0.08$). Thus, we cannot conclude on whether the difference
334 observed at DYFAMED/BOUSSOLE between the two periods is real or an artifact of
335 measurement techniques. As a sensitivity test, we compute the expected changes of DIC and
336 pH from 1995-1997 to 2013-2015 for a mean alkalinity increase of $10 \mu\text{mol kg}^{-1}$: we get
337 annual changes, $d\text{DIC}=+0.46 \mu\text{mol kg}^{-1} \text{ yr}^{-1}$ and $d\text{pH}=-0.0001 \text{ pH unit yr}^{-1}$, which are well
338 below errors estimated in section 3.4. Hence, such a change in alkalinity does not
339 significantly affect the increase of DIC and the decrease of pH shown in Table 2.

340

341 4.2 Drivers of the temporal change of DIC in surface waters

342 The increase in sea surface DIC from 1995-1997 to 2013-2015 is $25.2\pm 2.7 \mu\text{mol kg}^{-1}$ (Table
343 2). The expected contribution due to ocean uptake of anthropogenic CO_2 is $20.8\pm 1.3 \mu\text{mol}$
344 kg^{-1} . The difference between these two values is significant. In order to interpret this
345 difference, we examine potential changes that may result from interannual variability in local
346 physical and biological processes or anthropogenic carbon invasion from lateral advection of
347 Atlantic waters.

348 4.2.1 Natural variability

349 Time series of mixed layer depth, MLD, show a strong variability in winter at interannual
350 scale. During the two periods, 1995-1997 and 2013-2015, the winter MLD never exceeded
351 220 m, whereas values over 300 m were observed in 1999 and especially in February and
352 March 2006 with values close to 2000 m [Coppola et al., 2016; Pasqueron de Fommervault et
353 al., 2015]. These episodes of strong and deep vertical mixing must have entrained DIC rich

354 LIW in the surface waters. This could be causing an increase in DIC between the 1995-1997
355 and 2013-2015 periods. Monthly surface samples collected at the Dyfamed time series station
356 between 1998 and 2013 indicate an increasing DIC trend of $1.35 \mu\text{mol kg}^{-1} \text{yr}^{-1}$. This value is
357 known with great uncertainty ($r^2 = 0.05$) because of the large seasonal variability displayed in
358 the monthly samples [*Gemayel et al.*, 2015]. Nevertheless, this value is closer to the trend we
359 calculated between the two periods, 1993-1995 and 2013-2015 ($1.40 \mu\text{mol kg}^{-1} \text{yr}^{-1}$) than to
360 the trend inferred from the atmospheric increase ($1.15 \mu\text{mol kg}^{-1} \text{yr}^{-1}$). On DYPAMED time
361 series, we find no evidence that the strong increase in MLD observed during winters 1999 and
362 especially 2006 resulted in a further increase in DIC.

363 The monthly cruises of the Dyfamed time-series study have also been analyzed in order to
364 investigate the hydrological changes and some biological consequences over the period 1995-
365 2007 [*J. C. Marty and Chiavérini*, 2010]. These authors show that extreme convective mixing
366 events such as recorded in 1999 and 2006 are responsible of large increases in nutrient
367 content in surface layers and conclude that the biological productivity is increasing especially
368 during the 2003-2006 period, which could lead to a larger consumption of carbon, i.e. a
369 decrease of DIC.

370 4.2.2 Anthropogenic carbon exchange through the Strait of Gibraltar.

371 The concentration of oceanic anthropogenic carbon, C_{ant} , is not a directly measurable
372 quantity. To estimate it, several empirical methods have been developed. Flecha et al.[2012]
373 computed the anthropogenic carbon inventory in the Gulf of Cadiz. They used observations
374 made during a cruise in October 2008 throughout the oceanic area covered by the Gulf of
375 Cadiz and the Strait of Gibraltar to estimate C_{ant} with 3 methods: ΔC^* [*Gruber et al.*, 1996]
376 , TrOCA [*F Touratier and Goyet*, 2004; *F. Touratier et al.*, 2007] , ϕC_T^0 [*Vazquez-Rodriguez*
377 *et al.*, 2009]. In the 3 cases, their results indicate a net import of C_{ant} from the Atlantic
378 towards the Mediterranean through Gibraltar.

379 Schneider et al. [2010], using the transit time distribution method applied to a dataset of a
380 Mediterranean cruise in 2001, estimated a net anthropogenic carbon flux across the Strait of
381 Gibraltar into the Mediterranean Sea of 3.5Tg C yr^{-1} . Over the whole period from 1850 to
382 2001, this contribution of C_{ant} represents almost 10% of the total C_{ant} inventory of the
383 Mediterranean Sea. Accordingly, about 90% must have been taken directly by equilibrium
384 with atmospheric CO_2 . Based on a high-resolution regional model, Palmieri et al. [2015]
385 computed the anthropogenic carbon storage in the Mediterranean basin. They concluded that
386 75% of the total storage of C_{ant} in the whole basin comes from the atmosphere and 25% from
387 net transport from the Atlantic through the Strait of Gibraltar. The findings of these two

388 studies support our estimated change of DIC in excess of 17 \pm 10% over the direct
389 contribution of air-sea exchange suggesting that it could result from the anthropogenic carbon
390 input from the Atlantic Ocean towards the Mediterranean basin.

391 Huertas et al. [2009] and Schneider et al. [2010] report DIC_{ant} surface concentrations
392 respectively equal to 65-70 $\mu\text{mol kg}^{-1}$ at the Strait of Gibraltar in the years 2005-2007 and
393 close to 65 $\mu\text{mol kg}^{-1}$ in the western basin in 2001. We extrapolate these figures to the year
394 2014, assuming a mean increase rate of DIC equal to 1.4 $\mu\text{mol kg}^{-1}\text{yr}^{-1}$ as previously
395 computed (Table 2). Taking into account the increase of DIC_{ant} equal to 25.2 $\mu\text{mol kg}^{-1}$
396 between 1995-1997 and 2013-2015, we would estimate that the contribution of the change of
397 DIC_{ant} over the last 18 years represents \sim 30% of the total change since the beginning of the
398 industrial period ($t > \sim 1800$).

399

400 4.3 Long term trends in surface DIC and pH

401 The annual changes of DIC and pH_{SWS} calculated between 1995-1997 and 2013-2015 are
402 respectively equal to 1.40 \pm 0.15 $\mu\text{mol kg}^{-1}$ and -0.0022 \pm 0.0002. At the DYFAMED site, at
403 10 m, Marcellin Yao et al. [2016] studied the time variability of pH over 1995-2011, based on
404 measurements of T, S, Alk and DIC sampled approximately once a month. They computed a
405 mean annual decrease of -0.003 \pm 0.001 pH units on the seawater scale that is not
406 significantly different from our estimate. For the global surface ocean, Lauvset et al. [2015]
407 have reported a mean rate of decrease of pH, -0.0018 \pm 0.0004 for 1991-2011. This value is
408 also within the limits of uncertainty of the pH change computed in our study.

409 Bates et al. [2014] examined changes in surface seawater CO₂-carbonate chemistry at the
410 locations of seven ocean CO₂ time series that have been gathering sustained observations
411 from 15 to 30 years with monthly or seasonal sampling. Six stations are located in the
412 Atlantic and Pacific oceans in a latitudinal band between 10° N and 68°N. The range of
413 increasing and decreasing annual trends of DIC and pH extends from 0.93 \pm 0.24 to 1.89 \pm
414 0.45 $\mu\text{mol kg}^{-1}\text{yr}^{-1}$ and -0.0014 \pm 0.0005 to -0.0026 \pm 0.0006 respectively. The Revelle factor
415 of surfaces waters vary from 9-10 in the low latitude to 12-15 in the subpolar time series sites,
416 with higher Revelle factor values reflecting reduced capacity to absorb atmospheric CO₂. The
417 data show that the increase of DIC is not only controlled by the buffer capacity of the water
418 but compounding effects of changes in physical factors as strengthening of winter mixing or
419 larger air-sea uptake, have also to be taken into account [Olafson et al., 2010].

420 The increase of DIC computed at DYFAMED is rather in the upper range of values reported
421 at the other time series. A low Revelle factor, close to 10, characterizes the Mediterranean

422 Sea because of its warm and high-alkalinity waters. Moreover, as the result of a relatively
423 short deep water renewal time estimated to be 20-40 years in the western basin[*Schneider et*
424 *al.*, 2010] , the waters of the Mediterranean Sea have a relatively high absorption capacity to
425 absorb anthropogenic CO₂ from the atmosphere and transport it to depth.

426 The calculated decrease of pH in surface water at DYFAMED and in the global ocean are
427 quite similar, despite the higher alkalinity of the Mediterranean Sea. Thermodynamic
428 equilibrium calculations have highlighted the alkalinity effect on the Mediterranean
429 anthropogenic acidification [*Palmiéri et al.*, 2015]. Their results show that, notwithstanding a
430 higher total alkalinity, the average anthropogenic change in surface pH does not differ
431 significantly from the global average ocean.

432

433 **5 Conclusion**

434 High-frequency ocean fCO₂ measurements made by CARIOCA sensors were sufficient to
435 estimate trends in fCO₂, DIC and pH over a period of two decades, notwithstanding a
436 considerable short-time and natural seasonal variability of these properties at the sea surface.

437 We have estimated a large change of sea surface carbonate chemistry, an increase of DIC and
438 a decrease of pH. The computed increase of DIC is larger than the change expected from
439 chemical equilibrium with atmospheric CO₂. This could be the result of a strong interannual
440 variability of the winter mixing as observed between the two periods 1993-1995 and 2013-
441 2015. Likewise, our results support modeling work and analysis of vertical profiles
442 measurements that suggest that the Atlantic Ocean contributes as a source of anthropogenic
443 carbon towards the Mediterranean basin, close to 10% ([*Schneider et al.*, 2010] or 25%
444 [*Palmiéri et al.*, 2015]).

445

446 *Data availability:* Time series data from Dyfamed (1995-1997) are available in the SOCAT v3
447 database. Boussole data (2013-2015) will be available in SOCAT v6.

448

449 **Acknowledgments**

450 Seawater samples were analyzed for DIC and Alk by the SNAPO-CO₂ at LOCEAN in Paris.
451 The CO₂Sys toolbox of [*Pierrot et al.*, 2006] has been used for the calculations of DIC and
452 pH. The adaptation of CARIOCA sensors to high pressure has been supported by the BIO-
453 optics and CARbon EXperiment (BIOCAREX) project, funded by the Agence Nationale de la
454 Recherche (ANR, Paris). We are grateful for helpful comments from Gilles Reverdin on the
455 manuscript. Many thanks to Laurent Coppola who kindly provided additional MLD data at

456 Dyfamed.

457

458 **References**

459 Alvarez, M., H. Sanleon-Bartolome, T. Tanhua, L. Mintrop, A. Luchetta, C. Cantoni, K.
460 Schröder, and G. Civitarese (2014), The CO₂ system in the Mediterranean Sea: a basin
461 wide perspective, *Ocean Sci.*, 10, 69-92.

462 Antoine, D., F. d'Ortenzio, S. B. Hooker, G. Bécu, B. Gentili, D. Tailliez, and A. J. Scott
463 (2008), Assessment of uncertainty in the ocean reflectance determined by three satellite
464 ocean color sensors (MERIS, SeaWiFS and MODIS-A) at an offshore site in the
465 Mediterranean Sea (BOUSSOLE project), *Journal of Geophysical Research*, 113(C7).

466 Antoine., and others (2006), BOUSSOLE: A Joint CNRS-INSU,ESA, CNES and NASA ocean
467 color calibration and validation activity., *NASA Tech. Memo. 2006-214147*.

468 Bakker, D. C. E., et al. (2014), An update to the Surface Ocean CO₂ Atlas
469 (SOCAT version 2), *Earth Syst. Sci. Data*, 6(1), 69-90.

470 Bates, N., Y. Astor, M. Church, K. Currie, J. Dore, M. Gonaález-Dávila, L. Lorenzoni, F.
471 Muller-Karger, J. Olafsson, and M. Santa-Casiano (2014), A Time-Series View of Changing
472 Ocean Chemistry Due to Ocean Uptake of Anthropogenic CO₂ and Ocean Acidification,
473 *Oceanography*, 27(1), 126-141.

474 Begovic , M., and C. Copin-Montegut (2002), Processes controlling annual variations in
475 the partial pressure of fCO₂ in surface waters of the central northwestern
476 Mediterranean sea (Dyfamed site), *Deep-Sea Research II*, 49, 2031-2047.

477 Chen, G. T., and F. J. Millero (1979), Gradual increase of oceanic CO₂, *Nature*, 277, 205-
478 206.

479 Copin-Montegut, C., and M. Begovic (2002), Distributions of carbonate properties and
480 oxygen along the water column (0–2000 m) in the central part of the NW Mediterranean
481 Sea (Dyfamed site): influence of winter vertical mixing on air–sea CO₂ and O₂
482 exchanges, *Deep-Sea Research II* 49, 2049-2066.

483 Copin-Montégut, C., M. Bégovic, and L. Merlivat (2004), Variability of the partial pressure
484 of CO₂ on diel to annual time scales in the Northwestern Mediterranean Sea, *Mar Chem*,
485 85(3-4), 169-189.

486 Coppola, L., E. Diamond Riquier, and T. Carval (2016), Dyfamed observatory data,
487 *SEANOE*.

488 Dickson, A. G., and F. J. Millero (1987), A comparison of the equilibrium constants for the
489 dissociation of carbonic acid in seawater media, *Deep Sea Research Part A*.
490 *Oceanographic Research Papers*, 34(10), 1733-1743.

491 Dickson, A. G., C. L. Sabine, and J. R. Christian (2007), Guide to best practices for ocean
492 CO₂ measurements, *PICES Spec.Publ.3*, 176.

493 Edmond, J. M. (1970), High precision determination of titration alkalinity and total
494 carbon dioxide content of seawater by potentiometric titration, *Deep Sea research* 17(4),
495 737-750.

496 Flecha, S., F. F. Pérez, G. Navarro, J. Ruiz, I. Olivé, S. Rodríguez-Gálvez, E. Costas, and I. E.
497 Huertas (2012), Anthropogenic carbon inventory in the Gulf of Cádiz, *Journal of Marine*
498 *Systems*, 92(1), 67-75.

499 Gattuso, J.-P., and L. Hansson (2011), Ocean Acidification, *Oxford University Press*, 352
500 pp.

501 Gemayel, E., A. E. R. Hassoun, M. A. Benallal, C. Goyet, P. Rivaro, M. Abboud-Abi Saab, E.
502 Krasakopoulou, F. Touratier, and P. Ziveri (2015), Climatological variations of total

503 alkalinity and total dissolved inorganic carbon in the Mediterranean Sea surface waters,
504 *Earth System Dynamics*, 6(2), 789-800.

505 Gruber, N., J. L. Sarmiento, and T. F. Stocker (1996), An improved method for detecting
506 anthropogenic CO₂ in the oceans, *Global Biogeochem Cy*, 10, 809-837.

507 Heimbürger, L.-E., H. Lavigne, C. Migon, F. D'Ortenzio, C. Estournel, L. Coppola, and J.-C.
508 Miquel (2013), Temporal variability of vertical export flux at the DYFAMED time-series
509 station (Northwestern Mediterranean Sea), *Progress In Oceanography*, 119, 59-67.

510 Hood, E. M., and L. Merlivat (2001), Annual and interannual variations of fCO₂ in the
511 northwestern Mediterranean Sea: Results from hourly measurements made by CARIOCA
512 buoys, 1995-1997, *J Mar Res*, 59, 113-131.

513 Huertas, I. E., A. F. Ríos, J. García-Lafuente, A. Makaoui, S. ` Rodríguez-Gálvez, A. Sánchez-
514 Román, A. Orbi, J. Ruíz, and F. F. and Pérez (2009), Anthropogenic and natural CO₂
515 exchange through the Strait of Gibraltar, *Biogeosciences*, 6, 647-662.

516 Kapsenberg, L., S. Alliouane, F. Gazeau, L. Mousseau, and J.-P. Gattuso (2017), Coastal
517 ocean acidification and increasing total alkalinity in the northwestern Mediterranean
518 Sea, *Ocean Science*, 13(3), 411-426.

519 Lauvset, S. K., N. Gruber, P. Landschützer, A. Olsen, and J. Tjiputra (2015), Trends and
520 drivers in global surface ocean pH over the past 3 decades, *Biogeosciences*, 12(5), 1285-
521 1298.

522 Marcellin Yao, K., O. Marcou, C. Goyet, V. Guglielmi, F. Touratier, and J.-P. Savy (2016),
523 Time variability of the north-western Mediterranean Sea pH over 1995-2011, *Marine*
524 *Environmental Research*, 116, 51-60.

525 Marty, J. C., and J. Chiavérini (2010), Hydrological changes in the Ligurian Sea (NW
526 Mediterranean, DYFAMED site) during 1995-2007 and biogeochemical consequences,
527 *Biogeosciences*, 7(7), 2117-2128.

528 Marty, J. C., J. Chiaverini, M. Pizay, D., and B. Avril (2002), Seasonal and interannual
529 dynamics of nutrients and phytoplankton pigments in the western Mediterranean Sea at
530 the DYFAMED time-series station (1991-1999), *Deep-Sea Research II*, 49, 1965-1985.

531 McKinley, G. A., A. R. Fay, T. Takahashi , and N. Metzl (2011), Convergence of
532 atmospheric and North Atlantic carbon dioxide trends on multidecadal timescales,
533 *Nature Geoscience*, 4, 606-610.

534 Mehrbach, C., C. H. Culberson, J. E. Hawley, and R. M. Pytkowicz (1973), Measurement of
535 the apparent dissociation constants of carbonic acid in seawater at atmospheric
536 pressure, *Limnol Oceanogr*, 18(6), 897-907.

537 Merlivat, L., and P. Brault (1995), CARIOCA BUOY: Carbon Dioxide Monitor, *Sea*
538 *Technol*(October), 23-30.

539 Millero, F. J. (2007), The marine inorganic carbon cycle, *Chemical reviews*, 107(2), 308-
540 341.

541 Millot (1999), Circulation in the Western Mediterranean Sea, *Journal of Marine Systems*,
542 20, 423-442.

543 Olafson, J., S. Olafsdottir, A. Benoit-Cattin, and T. Takahashi (2010), The Irminger Sea and
544 the Iceland Sea time series measurements of sea water carbon and nutrient chemistry
545 1983-2008, *Earth Syst. Sci. Data*, 2, 99-104.

546 Palmiéri, J., J. C. Orr, J. C. Dutay, K. Béranger, A. Schneider, J. Beuvier, and S. Somot
547 (2015), Simulated anthropogenic CO₂ storage and acidification of the Mediterranean
548 Sea, *Biogeosciences*, 12(3), 781-802.

549 Pasqueron de Fommervault, O., C. Migon, F. D'Ortenzio, M. Ribera d'Alcalà, and L.
550 Coppola (2015), Temporal variability of nutrient concentrations in the northwestern

551 Mediterranean sea (DYFAMED time-series station), *Deep Sea Research Part I:*
552 *Oceanographic Research Papers*, 100, 1-12.

553 Pierrot, D., E. Lewis, and D. W. R. Wallace (2006), MS excel program developed for CO2
554 system calculations, *In: Carbon Dioxide Information Analysis Center (ed.O.R.N.L.).*
555 *US.Department of Energy, Oak Ridge, TN.*

556 Sabine, C. L., R. A. Feely, F. J. Millero, A. G. Dickson, C. Langdon, S. Mecking, and D. Greeley
557 (2008), Decadal changes in Pacific carbon, *J.Geophys.Res.*, 113(C07021).

558 Schneider, A., T. Tanhua, A. Körtzinger, and D. W. R. Wallace (2010), High anthropogenic
559 carbon content in the eastern Mediterranean, *Journal of Geophysical Research*, 115(C12).

560 Takahashi , T., J. Olafson, J. G. Goddard, D. W. Chipman , and G. Sutherland (1993),
561 Seasonal variations of CO2 and nutrients in the high-latitude surface oceans:a
562 comparative study, *Global Biogeochem Cy*, 7(4), 843-878.

563 Touratier, F., and C. Goyet (2004), Applying the new TrOCA approach to assess the
564 distribution of anthropogenic CO2 in the Atlantic Ocean, *Journal of Marine Systems*, 46(1-
565 4), 181-197.

566 Touratier, F., and C. Goyet (2009), Decadal evolution of anthropogenic CO2 in the
567 northwestern Mediterranean Sea from the mid-1990s to the mid-2000s, *Deep Sea*
568 *Research Part I: Oceanographic Research Papers*, 56(10), 1708-1716.

569 Touratier, F., L. Azouzi, and C. Goyet (2007), CFC-11, $\delta^{14}\text{C}$ and $\delta^3\text{H}$ tracers as a means to
570 assess anthropogenic CO2 concentrations in the ocean, *Tellus B*, 59(2), 318-325.

571 Vazquez-Rodriguez, M., X. A. Padin, A. F. Rios, R. G. J. Bellerby, and Perez.F.F. (2009), An
572 upgraded carbon-based method to estimate the anthropogenic fraction of dissolved CO2
573 in the Atlantic Ocean, *Biogeosciences Discussions*, 6, 4527-4571.

574 Woosley, R. J., F. J. Millero, and R. Wanninkhof (2016), Rapid anthropogenic changes in
575 CO2 and pH in the Atlantic Ocean: 2003-2014, *Global Biogeochem Cy*, 30(1), 70-90.

576
577

577

578

Table 1:

579

580 Distribution of temperature, fCO₂@13, and increase dfCO₂@13 data binned by 1°C

581 temperature interval for the 2 periods 1995-1997 and 2013-2015 .

582 The mean temperature within each 1° step differ for the two periods as the distribution of

583 individual measurements are not identical.

584

585

Time interval 1995-1997				Time interval 2013-2015				Temporal change	
T ^l	fCO ₂ @13	N	standard deviation	T ^l	fCO ₂ @13	N	standard deviation	dfCO ₂ @13	standard deviation
°C	µatm		µatm	°C	µatm		µatm	µatm	µatm
13.45	331.58	1212	28.09	13.55	363.14	6869	18.07	31.56	33.40
14.45	305.28	495	26.02	14.43	337.16	3270	16.65	31.87	30.89
15.37	281.54	447	9.62	15.57	321.10	3112	11.09	39.56	14.68
16.44	274.43	182	8.53	16.42	313.79	1818	11.09	39.36	13.99
17.58	275.54	190	7.04	17.56	306.83	1528	14.65	31.29	16.25
18.47	277.34	300	9.04	18.45	296.57	2621	10.95	19.23	14.20
19.62	265.43	342	15.58	19.41	291.84	1406	13.45	26.40	20.59
20.50	258.08	529	14.15	20.50	293.16	1135	18.21	35.08	23.06
21.56	271.15	239	12.98	21.54	297.96	1200	20.41	26.82	24.19
22.49	250.75	742	13.66	22.49	290.27	2385	18.57	39.52	23.05
23.57	252.22	320	13.00	23.47	296.92	747	21.77	44.70	25.36
24.41	245.85	506	7.08	24.40	280.44	959	14.82	34.59	16.43
25.50	250.06	215	10.77	25.53	284.05	456	14.81	33.99	18.31
26.42	256.29	279	6.24	26.29	286.71	249	11.23	30.42	12.85

586

587

588

589

590
591
592
593
594
595
596
597
598
599

Table 2

Seasonally detrended long term and annual trends of seawater carbonate chemistry and atmosphere composition.

T, mean annual temperature equal to 18.25°C

*, Change from 1995-1997 to 2013-2015.

**, dDIC_{ant}

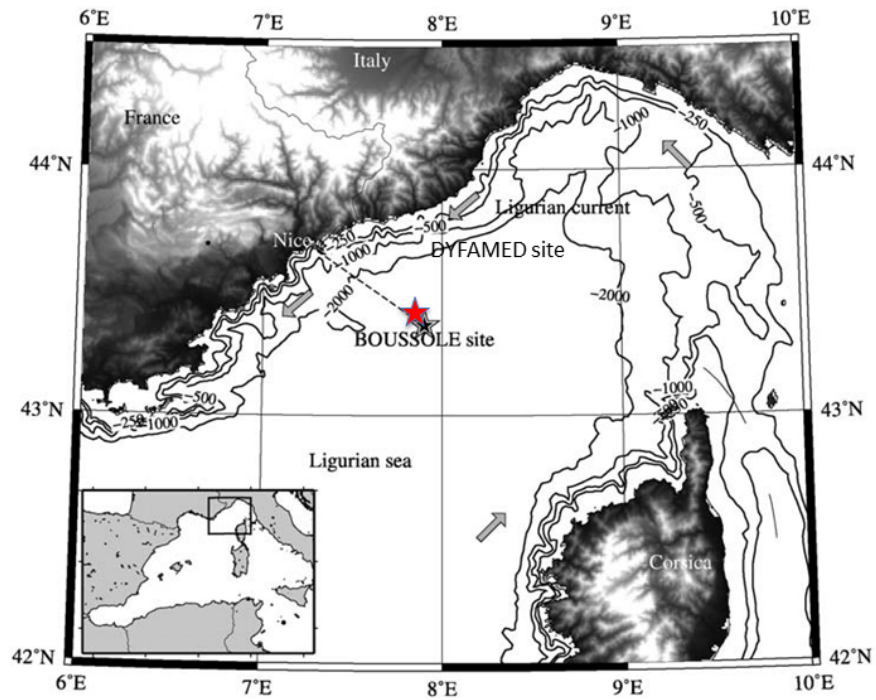
***, dpH_{SWS} computed at T

	d fCO ₂ [*] @ 13 µatm	d fCO ₂ [*] @ T µatm	d DIC [*] µmolkg ⁻¹	d pH _{SWS} ^{***} pH unit	dfCO ₂ @T annual µatm yr ⁻¹	d DIC annual µmolkg ⁻¹ yr ⁻¹	d pH _{SWS} ^{***} annual pH unit yr ⁻¹
sea surface	33.2 +/-3.3	41.4 +/-4.1	25.2 +/-2.7	-0.0397 +/-0.0042	2.30 +/-0.23	1.40 +/-0.15	-0.0022 +/-0.0002
atmosphere Lampedusa data		34.3 +/-2.3	**20.8 +/-1.3		1.91 +/-0.13	1.15 +/-0.07	
dfCO ₂ @T _{air} /dfCO ₂ @T _{sea}		0.83 +/-0.10	0.83 +/-0.09				

600
601
602
603
604
605
606
607
608
609
610
611
612
613
614
615

616
617
618
619
620
621

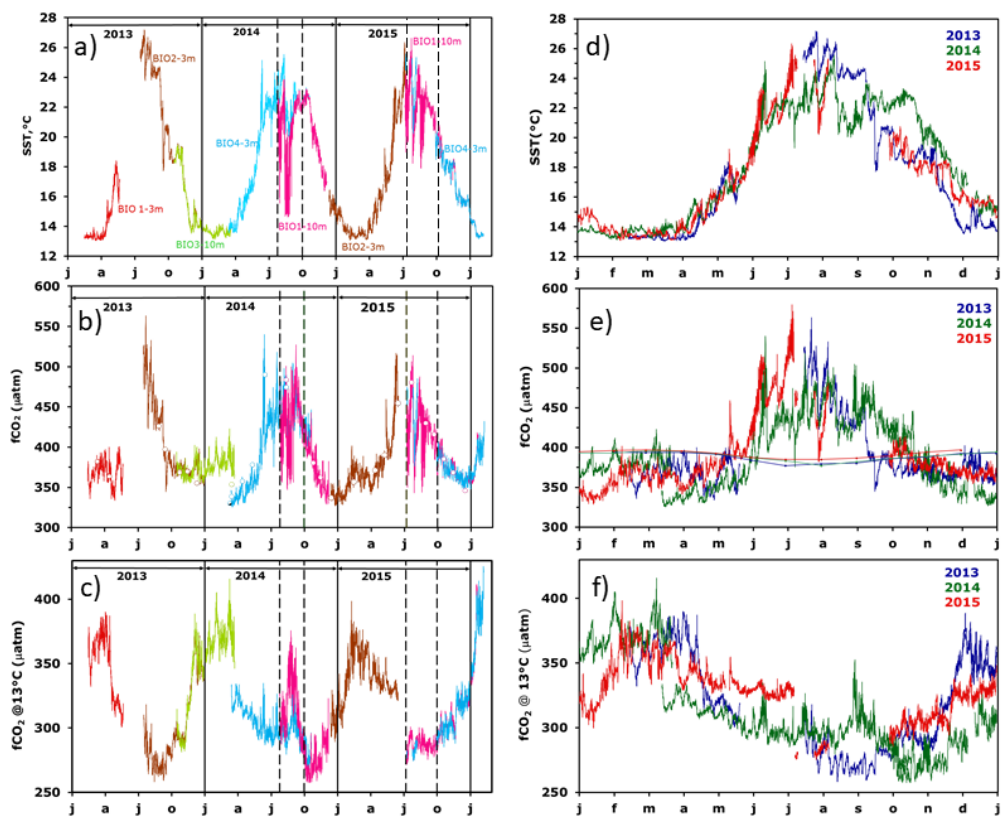
Figure 1. The area of the northwestern Mediterranean Sea showing the southern coast of France, the Island of Corsica, the main current branches (gray arrows), and the location of the DYFAMED site (43°25'N, 7°52'E, red star) and the BOUSSOLE buoy (43°22'N, 7°54'E, black star) in the Ligurian Sea.



622
623
624
625
626
627
628
629
630
631
632
633

634
635
636
637
638
639
640
641

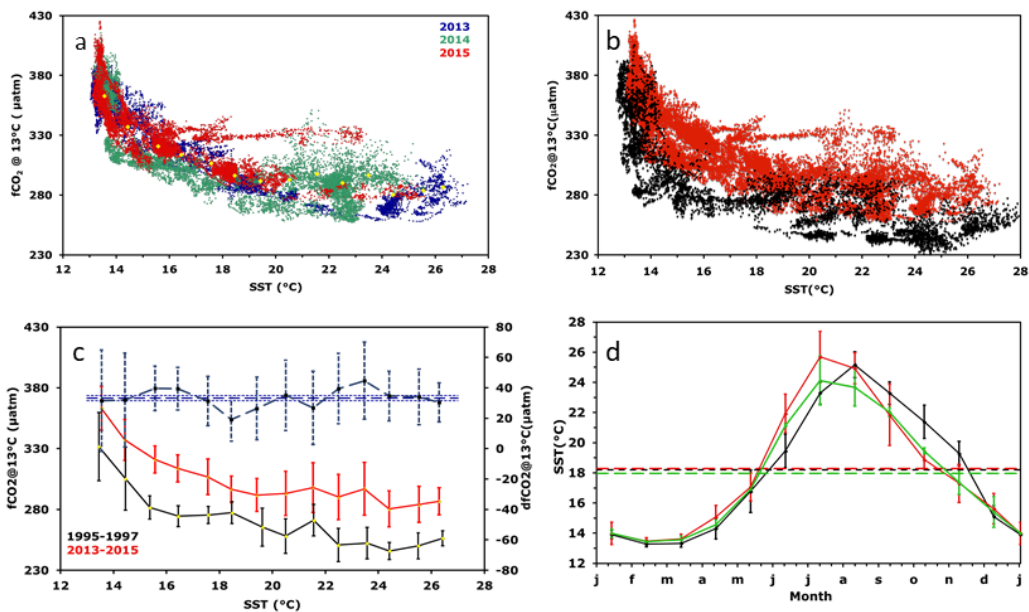
Figure 2. Interannual variability of CARIOCA data: a) T, b) $f\text{CO}_2$, c) $f\text{CO}_2@13$. The dotted lines indicate the period affected by stratification and internal waves (July, 26th to October 1st, 2014 and July, 8th to October 1st, 2015). On 2(b), the open circles correspond to $f\text{CO}_2$ data derived from DIC and alkalinity measurements of samples taken at 5 and 10 m. (d), (e), (f), seasonal variability. On 2(e), the thin lines indicate $f\text{CO}_{2\text{atm}}$. Note that the color code on (d), (e), (f) is different from (a), (b), (c).



642
643
644
645
646
647
648
649
650
651

652
653
654
655
656
657
658
659
660
661

Figure 3. (a) $fCO_2@13$ as a function of temperature for hourly data in 2013, 2014 and 2015. The yellow dots indicate mean $fCO_2@13$ (b) as in (a) but for all hourly data in 1995-1997 (black) and in 2013-2015 (red) (c) As in (b), but for average values per $1^\circ C$ interval (standard deviation as dotted line). The difference between the two periods is also displayed (dashed black curve; scale on the right axis). (d) Mean monthly sea surface temperature for 1993-1995 (black curve; CARIOCA sensors), 2013-2015 (green; CARIOCA sensors), 2013-2015 (red, meteorological buoy). Corresponding mean annual values are indicated by dotted lines.



662
663